## Localizing the Ising CFT from the ground state of the Ising model on the fuzzy sphere

## Kay Jörg Wiese

CNRS-Laboratoire de Physique de l'Ecole Normale Supérieure, PSL Research University, Sorbonne Université, Université Paris Cité, 24 rue Lhomond, 75005 Paris, France.

October 9, 2025 - FuzzyGroundstate-arXiv1.tex - compilation 15

We locate the phase-transition line for the Ising model on the fuzzy sphere from a finite-size scaling analysis of its ground-state energy. This is similar to what was used to locate the complex CFT of the 5-state Potts model in dimension d=2 [PRL 133 (2024) 077101]. There it was shown that a CFT is characterized by a stationarity condition for the measured effective central charge. Our strategy is to write the ground-state energy as  $E_{\rm GS}(N)/N_m=E_0+E_1/N_m+E_{3/2}/N_m^{3/2}+...$ , and to search for a minimum of  $E_{3/2}/E_0$  as a function of the couplings. This procedure finds the critical curve of [PRX 13 (2023) 021009] with good precision, and their sweet spot as well. We find similar results when normalizing by the gap to the stress tensor or first parity-odd singlet.

## I. INTRODUCTION

The fuzzy-sphere regularization is an exciting new tool [1] to access conformal field theories (CFTs) in dimension d=2+1. The technique uses a 2-sphere inside which are placed s magnetic monopoles. The lowest Landau level on this sphere is  $N_m = 2s+1$  times degenerate, each with  $N_{\rm f}$  flavors ( $N_{\rm f}=2$  for the Ising model). Filling  $N_m$  of the  $N_m\times N_{\rm f}$ states, and adding interactions between the electrons, allows one to engineer CFTs with a given symmetry. This approach was introduced in [1] to study the quantum 2d Ising model, equivalent to the classical 3d Ising model. It was since applied to other systems, among which are theories with Sp(n)global symmetry [2], Chern-Simons matter [3] and the Potts model [4–7]. The last example is interesting as the theory is non-unitary, even though its spectrum is real; thus it is not accessible via the numerical conformal bootstrap [8–12], which is the current gold standard for 3d CFTs.

While the method allows one to study phases as well as critical points, the latter are particularly interesting, especially when they correspond to a CFT. A crucial step is to identify the location of the critical point. The standard approach consists in choosing couplings which optimize properties of the intended CFT. Doing so without assuming what one wants to show is critical. There are interesting recent proposals [13, 14] to construct the conformal generators on the fuzzy sphere, allowing one to check for the overlap of states conjectured to be descendants, with the constructed descendant of known primaries.

Here we locate the phase-transition line and sweet spot for the Ising model on the fuzzy sphere from a finite-size scaling analysis of the ground-state energy, without using any information on higher excited states. Our procedure finds the critical curve of [1] with good precision, and their sweet spot (point of optimal conformality) as well.

# II. SIZE-DEPENDENCE OF THE GROUND STATE ENERGY

In dimension d = 2, the free energy per site of a CFT on a torus of circumference L is given by [15, 16],

$$f = f_{\infty} - \frac{\pi c_{\text{eff}}}{6L^2} + \mathcal{O}(L^{-3}).$$
 (1)

Here  $f_{\infty}$  is the free energy per site in the limit of  $L \to \infty$ , and  $c_{\text{eff}}$  the effective central charge. This formula is valid at the critical point, and can be used to locate it: one demands that the theory is at a marginal point for the measured effective central charge [17],

$$\partial_g c_{\text{eff}}(g)\big|_{g=g^*} = 0 \qquad \Longrightarrow \qquad c_{\text{eff}}(g^*) = c_{\text{CFT}}.$$
 (2)

For a standard (real) CFT, a local minimum for  $c_{\rm eff}$  indicates a critical point, while a local maximum for  $c_{\rm eff}$  indicates a tricritical point. If the microscopic model is a CFT, then  $c_{\rm eff}(g^*)$  is the central charge of the corresponding CFT.

The central charge has three properties: (i) it appears in the Virasoro algebra of conformal generators, (ii) it governs finite-size corrections as in Eq. (1), and it decreases along the RG flow (Zamolodchikov's c-theorem [18]). This motivates the condition (2) for IR attractive fixed points, and explains why a critical point is a local minimum, and a tricritical point a local maximum. The marginality condition (1) can also be used for complex CFTs, and allowed the authors of [17] to locate the critical point of the 5-state Potts model in d=2, which has a complex second derivative, thus is neither maximum nor minimum.

The author wondered whether a similar procedure may be available in higher dimensions. There is a generalization of Zamolodchikov's c-theorem to d=4, related to anomalies under Weyl rescaling [19, 20], which gives the stress-energy tensor in the form (see Eq. (1.2) of [21])

$$T^{\mu}_{\mu} = aE_4 - cW^2_{\mu\nu\rho\sigma}.\tag{3}$$

Here  $E_4$  is the Euler density (which integrates to the Euler characteristic), and W the Weyl tensor. It was first conjectured and checked to 1-loop order by Cardy [22], and later proven in [21] that a decays along RG trajectories (a-theorem). There is, however, a caveat for practical applications: on a sphere the Euler-characteristics vanishes, and a inaccessible. How to extract it from the entanglement entropy was shown in [23].

We now consider dimension d=3. Ref. [24] (section 1) considers finite-size corrections for an Euclidean field theory on a 3-sphere of radius R imbedded into  $\mathbb{R}^4$ ,

$$F = -\ln|Z_{S^3}| = \alpha_1 R^3 + \alpha_2 R + \mathcal{F}.$$
 (4)

 $\mathcal{F}$  was first obtained via holography [25] and in supersymmetric models [26], and only later for more general theories [27]. It took some time to find a proper definition of  $\mathcal{F}$  which is universal, and independent of the microscopic degrees of freedom [28, 29]. Currently, the best approach to extract  $\mathcal{F}$  is to study the entanglement spectrum [30]. Refs. [29, 30] proved that  $\mathcal{F}$  so defined descends along the RG flow. For the fuzzy sphere Ref. [31] succeeded to apply this to the Ising model. Splitting the sphere at latitude  $\theta$  (parallel to the equator), the entanglement entropy  $S_A(\theta)$  reads [31]

$$S_A(\theta) = \alpha \frac{R}{\delta} \sin \theta - \mathcal{F}. \tag{5}$$

To our knowledge, no relation to finite-size corrections is known.

*Inspired* by Eq. (4), our strategy is to write the ground-state energy per electron<sup>1</sup> as

$$\frac{E_{\rm GS}(N_m)}{N_m} = E_0 + \frac{E_1}{N_m} + \frac{E_{3/2}}{N_m^{3/2}} + \dots$$
 (6)

and to look for a minimum of  $E_{3/2}/E_0$  as a function of the couplings. We wrote "inspired" as there is no obvious relation between Eq. (4) derived for a 3-sphere imbedded into  $\mathbb{R}^4$  and the fuzzy sphere. We are comforted in our choice by the observation that the stress-energy tensor gap  $E_T-E_{\rm GS}$  has the same scaling in  $N_m$  as  $E_{3/2}$  (see discussion below and Fig. 7); thus if one looks for a coefficients of the ground-state energy which is universal, the only viable candidate is  $E_{3/2}$ .

As we shall show, this procedure finds the critical curve and the sweet spot of [1] with good precision. The standard algorithm to locate a CFT is to search for a spectrum with integer-valued spacing for descendants of primary operators, as dictated by CFT [1], or explicitly check for conformal symmetry [13, 14]. Our procedure is an alternative. Its sole ingredient is the ground-state energy, and no further assumptions are made. Its advantages are that it is simple to implement, and computationally fast.

## III. FINITE-SIZE SCALING ANALYSIS OF THE GROUND-STATE ENERGY

#### A. Model

We use the Ising model defined in the seminal work [1]. It consists of a 2-sphere with s magnetic monopoles at its center, and onto which are placed  $N_m=2s+1$  fermions, each with two internal degrees of freedom (up and down spin). Without interactions, the spectrum is flat. One then introduces a repulsive interaction upon contact between electrons pointing in the z-direction of strength 1, and a "kinetic" term (coupling

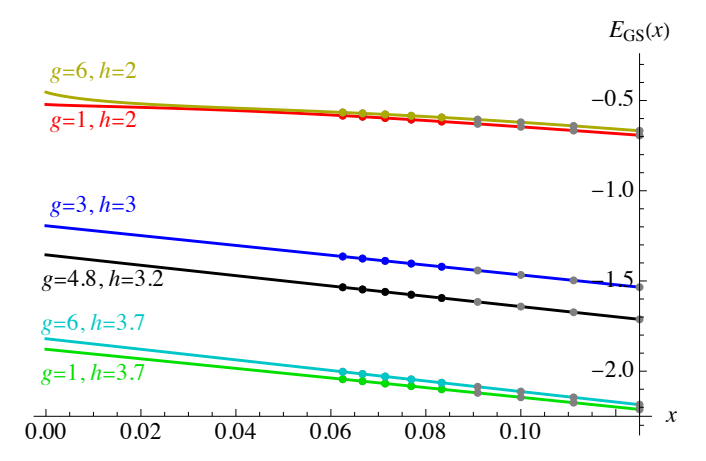


FIG. 1.  $E_{\rm GS}(x)$  for various values of h and g, for o=4, using  $x^{i/2}$  as a basis,  $\{1,x,x^{3/2},x^2,x^{5/2}\}$ ,  $N_m^{\rm max}=16$ . Gray dots are not used for the fit, but in agreement with it.

to the gradient of the density interactions) of strength g in the same direction. Finally, a transverse magnetic field of strength h drives the phase transition, similar to what happens in the 1-dimensional spin chain.

## B. FuzzifiED

We use the package FuzzifiED. It provides a compact and efficient implementation to obtain the spectrum of a user-defined model on the fuzzy sphere, both using exact diagonalization and DMRG. The package is described in detail in [32]. The program used is an adaptation of "ising\_spectrum.jl", wrapped inside a Mathematica loop. To avoid numerical errors, we eliminated the rounding, i.e. the instruction "round.([enrg[i], 12-val[i], P, Z], digits = 6)". For system sizes  $N_m \geq 16$  we restrict the evaluation to the ground-state energy, leading to a considerable speedup. (We can do  $N_m = 17$  in about 10 minute on 8 cores, using a machine from 2013.)

## C. Dependence of the ground-state energy on system size

We use the identification that the area of the sphere grows as the number of electrons, or more precisely [32]

$$N_m^2 = 1 + 4R^4. (7)$$

Fig. 1 shows that as a function of

$$x := \frac{1}{N_m} \simeq \frac{1}{2R^2},\tag{8}$$

the energy of the ground-state<sup>1</sup> has a strong linear component. The question is what the best ansatz is. A simple polynomial fit would be

$$\frac{E_{GS}(x|h,g)}{N_m} = \sum_{i=0}^{o} E_i(h,g)x^i.$$
 (9)

<sup>&</sup>lt;sup>1</sup> The ground-state energy given by FuzzifiED is  $\sim N_m$ . What we report here is the energy per electron, obtained by dividing by  $N_m$ .

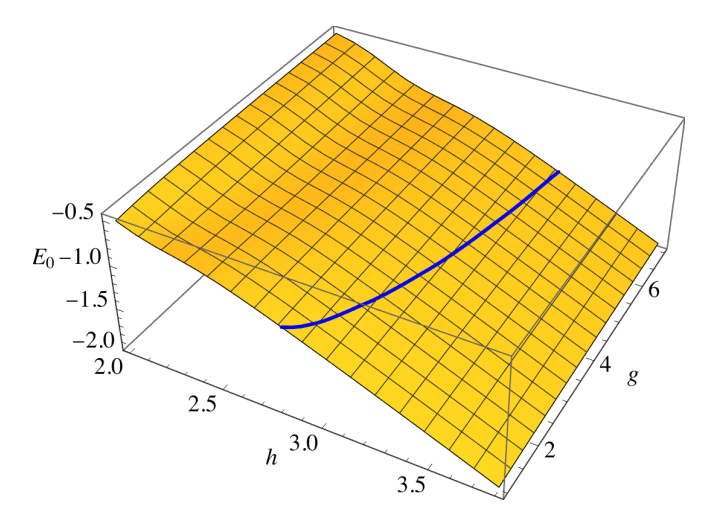


FIG. 2.  $E_0=E_{\rm GS}(0|h,g)$  for o=4,  $N_m^{\rm max}=16$ ; this plot changes little between  $N_m^{\rm max}=13$  and  $N_m^{\rm max}=16$ . In blue the critical line.

The alternative used by [4] is

$$\frac{E_{GS}(x|h,g)}{N_m} = \sum_{i=0}^{o} E_{i/2}(h,g)x^{\frac{i}{2}}.$$
 (10)

We have experimented with the fits (9) (in powers of x), and (10) in powers of  $1/R \simeq \sqrt{2x}$ . For fits with integer powers the information about the critical line seems to be sitting in higher derivatives, which we do not find convincing, see appendix A.

Our final choice suggested by Eq. (4) and stated in Eq. (6) is

$$\frac{E_{\text{GS}}(x|h,g)}{N_m} = E_0(h,g) + E_1(h,g)x + E_{3/2}(h,g)x^{\frac{3}{2}} + E_2(h,g)x^2 + E_{5/2}(h,g)x^{\frac{5}{2}} + \dots$$
(11)

Our protocol is to obtain  $E_{\rm GS}(x=1/N_m|h,g)$ , fit this to available system sizes, by choosing the largest possible sizes so that all coefficients are fixed. We played with different orders o of truncation. We trust our analysis when higher-order coefficients are small. With its almost straight behavior, Fig. 1 (which uses o=4) suggests that the leading term in the expansion is indeed of order x, and not  $\sqrt{x}$ , or that at least the coefficient  $\sim \sqrt{x}$  is very small. This, the predicted form (4) (on  $S_3 \subset \mathbb{R}^4$ ), as well as its absence in dimension d=2, see Eq. (1), led us to discard the term  $\sim \sqrt{x}$ .

We now look at the GS energy extrapolated to x=0. As Fig. 2 attests this is rather featureless. A crucial problem with quantum-mechanical approaches is that all energy levels are multiplied by an unknown Fermi velocity. In the fuzzy-sphere approach, this is usually fixed by demanding that the stress-energy tensor have dimension d=3. An alternative is to prescribe the energy of the first excited state  $\sigma$  which suffers less from finite-size corrections close to the Ising CFT [33]. Our goal here is to extract the location of the CFT solely from the ground-state energy. To eliminate the unknown Fermi-velocity, we consider finite-size corrections normalized by the

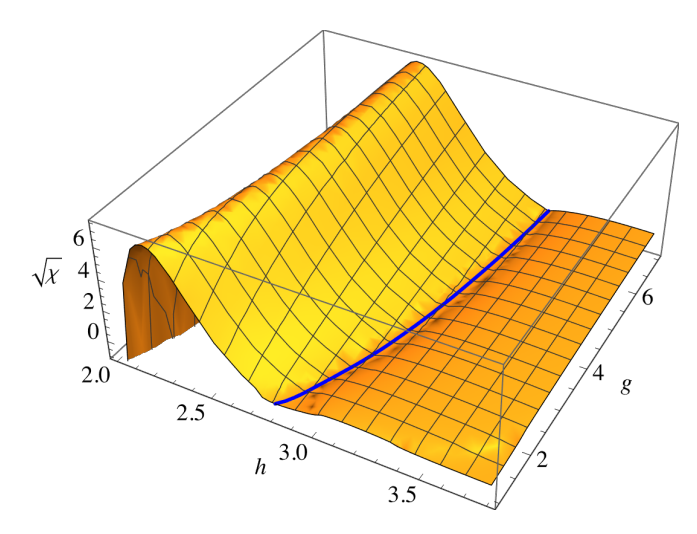


FIG. 3.  $\chi$  for  $N_m^{\rm max}=16$ ; in blue the critical line. To make the minimum visible, we plot the signed root  $(\sqrt{\chi}:={\rm sign}(\chi)\sqrt{|\chi|})$ . To enhance the resolution of the plot, the interpolation outlined below in Eq. (13) and Fig. 5 was used.

extrapolated ground-state energy, i.e.

$$\chi(h,g) := \frac{E_{3/2}(h,g)}{E_0(h,g)},\tag{12}$$

where the coefficients are those of Eq. (11).

## D. Implementation

Our ED data are such that we can use  $N_m=8$  to 17, i.e. a maximal  $N_m$  per fit of  $N_m^{\rm max}=12$  to 17. Large sizes are possible since we only need the GS energy. For the order of approximation, we tried o=2,3,4,5 and 6. Larger orders o are not necessarily better, as numerical artifacts are amplified in ways possibly not detectable. Common sense and experience lead us to consider o=4 optimal, i.e. the form given in Eq. (11).

We now evaluate  $\chi$ : following [1], we plot h on the horizontal axis, and g on the vertical axis. We first show a 3D plot, see Fig. 3, then a heat-plot on Fig. 4. On the latter, the critical line of [1] is given in white (partially hidden under blue dots), with a white shamrock marking their *sweet spot* (best agreement with Ising CFT). The dark blue dots in Fig. 4 mark the valley floor, defined as follows: look at the Hessian  $H_{ij} := \partial_i \partial_j \chi(h,g)$ , where  $i,j \in \{h,g\}$ . Since  $H_{ij}$  is symmetric, it has two eigenvalues, the curvatures, and two eigenvectors, which are orthogonal. We take the eigenvector in the direction of the larger curvature, and ask that the slope in this direction vanishes<sup>2</sup>.

<sup>&</sup>lt;sup>2</sup> This definition uses the metric of the coordinates h and g. It is not invariant under reparametrization, e.g.  $\{h,g\} \rightarrow \{h,g+h\}$ . The result is rather similar if we look at a vanishing slope in the h direction only; this we believe is what [1] did in their optimization procedure.

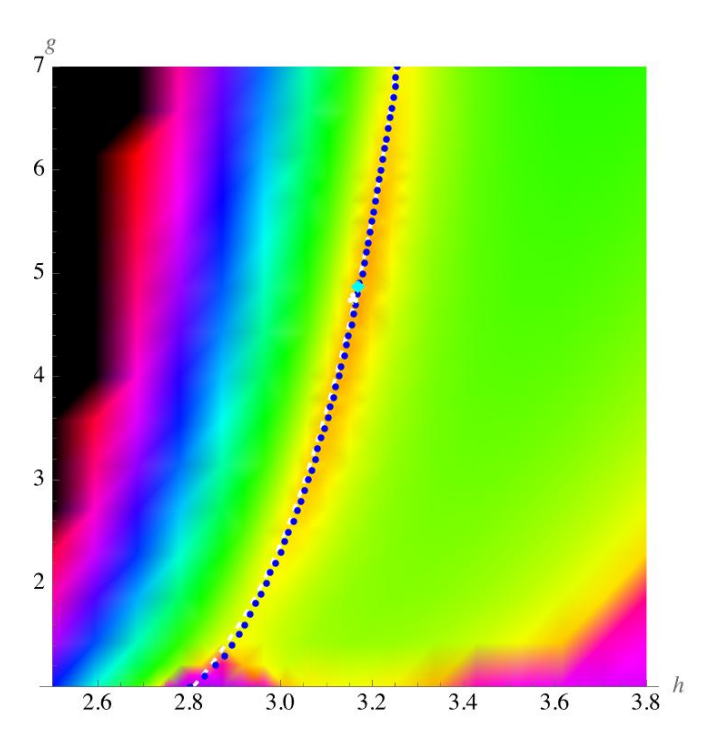


FIG. 4. Heat map of  $\chi(h,g)$  given in Eq. (12) for o=4,  $N_m^{\rm max}=16$ . The white dashed line is the critical line of [1], with a white shamrock marking their sweat spot (best agreement with a CFT). In dark blue dots the minimum of the valley of  $\chi(h,g)$ . The cyan diamond marks the global minimum of  $\chi(h,g)$ .

This is a highly non-linear operation on the numerical data generated on a grid with step size  $\delta h=1/20,\,\delta g=1/5,$  for which we need a smooth interpolation. This is obtained by fitting a polynomial of maximal degree four (15 coefficients) to the  $6\times 6$  neighbors, weighted by

$$\rho(h,g) := \exp\left(-\alpha \left[\frac{(h_i - h)^2}{\delta h^2} + \frac{(g_i - g)^2}{\delta g^2}\right]\right), \quad (13)$$

where  $\alpha=0.6$  is a phenomenological parameter. An example for the weights is given on Fig. 5. Compared to lattice-based approaches which are discontinuous when a new interpolation point enters, our procedure is very smooth. If the data turn out to be noisy, one can decrease  $\alpha$  to effectively include more points in the fit. The number of neighbors is chosen s.t. additional points have vanishing weight.

## E. Results for the location of the critical point

As Fig. 4 attests, we can localize the phase-transition line of Ref. [1] which corresponds to the white dashed line. Our valley of  $\chi(h,g)$  is marked by blue dots. On this phase-transition line the best agreement with the Ising CFT is achieved at the position of the white shamrock [1], while the nearby global minimum of  $\chi(h,g)$  is marked by a cyan diamond. The latter minimum satisfies

CFT: 
$$\partial_h \chi(h, g) = \partial_g \chi(h, g) = 0.$$
 (14)

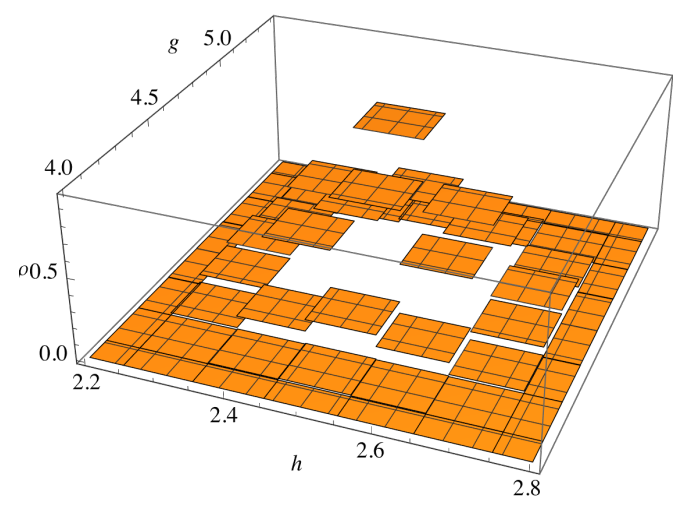


FIG. 5. The weights  $\rho(h,g)$  defined in Eq. (13), for h=2.5 and g=4.75 (off grid).

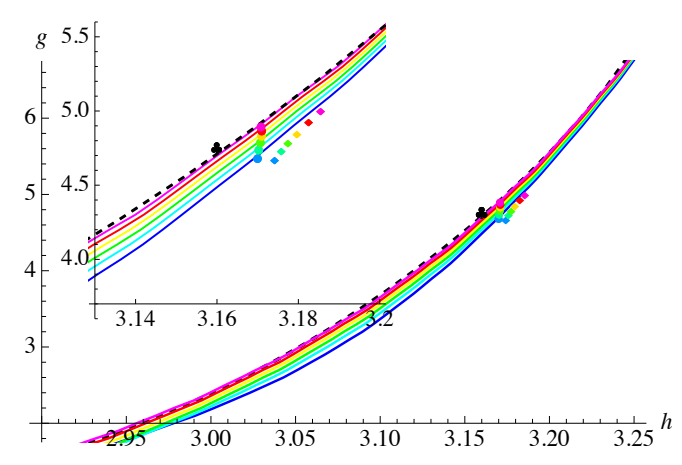


FIG. 6. Main plot: Dependence on  $N_m^{\rm max}$  of the critical curve and sweet spot (dots) from a grid with  $\delta g=0.2$ ,  $\delta h=0.05$ ; from  $N_m^{\rm max}=12$  (blue), over  $N_m^{\rm max}=13$  (cyan) to  $N_m^{\rm max}=17$  (magenta); diamonds mark the minimum on a micro-grid with discretization  $\delta g=0.05$ ,  $\delta h=0.01$ . The inset shows a blow-up around the sweet spot. Deviations are indicative of errors due to the finite grid size. In black dashed the critical line of [1], a black trefle marking its sweet spot.

How this minimum depends on the system size is shown in Fig. 6. There is a small systematic upwards drift on the minima obtained via interpolation (dots). We repeated the analysis on a much finer grid ("micro-grid") with  $\delta g=0.05$  and  $\delta h=0.01$  around the sweet spot, obtaining comparable results, see the diamonds on Fig. 6, and table I.

#### F. Different normalizations

The alert reader will object that  $E_0$  is not universal. We propose two ways out of the dilemma, which demand to calculate one more eigen value, either  $E_T$ , the subleading contribution

$N_m^{\max}$	h	g	χ
12	3.17422	4.66314	0.00564418
13	3.17587	4.72479	0.00543531
14	3.17750	4.78087	0.00500998
15	3.17965	4.84383	0.00455052
16	3.18256	4.91919	0.00411340
17	3.18553	4.99396	0.00371342

TABLE I. Values for the minimum of  $\chi$  and its location for different  $N_m^{\rm max}$ , obtained on a grid with  $\delta g = 0.05$ ,  $\delta h = 0.01$ .

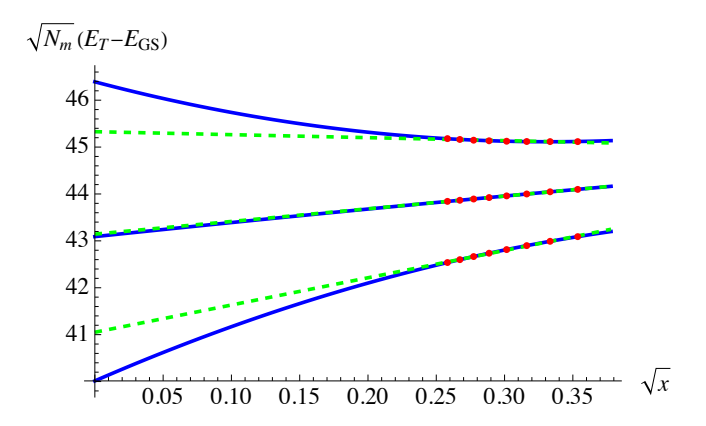


FIG. 7. The rescaled stress-energy tensor gap  $\sqrt{N_m}(E_T-E_{\rm GS})$  ( $\ell=2,\,P=Z=1$ ) close to the sweet spot: g=4.8 and h=3.1 (bottom), h=3.2 (middle), h=3.3 (top). Fits to  $\{1,\sqrt{x},x\}$  (blue), compared to a linear fit (dashed green line). Interestingly, the curvature changes sign at the transition.

in the GS sector corresponding to the stress-energy tensor, or  $E_{\sigma}$ , the lowest-lying parity-odd state.

Let us first consider  $E_T$ . On Fig. 7 we show how weakly  $E_T-E_{\rm GS}$  depends on x. We found it appropriate to fit to  $\{1,\sqrt{x},x\}$ . Interestingly, the curvature changes sign at the transition; one should explore this further. Fig. 8 shows the resulting extrapolated value of the stress-energy gap as a function of h and g. This allows us to define

$$\chi_T := \frac{E_{3/2}}{\sqrt{N_m}(E_T - E_{GS})}.$$
 (15)

A plot of this function is shown on Fig. 9, which should be compared to Fig. 3.

An alternative is to normalize by the gap of the first parityodd operator  $\sigma$ ,

$$\chi_{\sigma} := \frac{E_{3/2}}{\sqrt{N_m}(E_{\sigma} - E_{GS})}.$$
(16)

While the  $\sigma$ -gap is rather insensitive to perturbations close to the Ising CFT [33], it depends strongly on h, as Fig. 10 attests. Trying to extrapolate to  $N_m = \infty$  even with a linear fit in  $\sqrt{x}$  and two consecutive system sizes leads to a non-sensical negative gap. For this reason, we use only one system size for the normalization in Eq. (16). The result is shown on Fig. 11, which should be compared to Figs. 3 and 9.

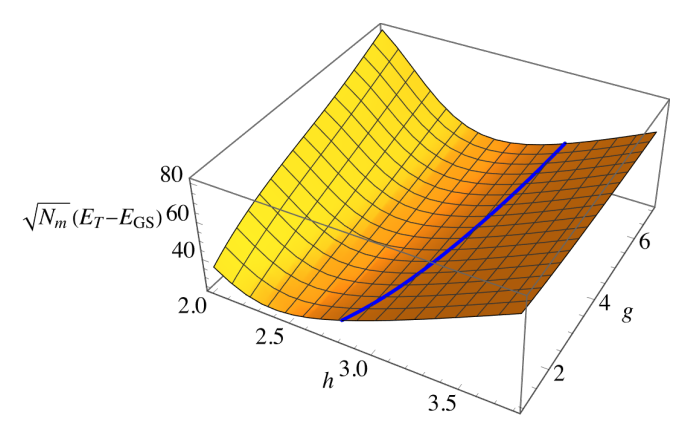


FIG. 8. The stress-energy tensor gap  $(\ell=2, P=Z=1)$  multiplied by  $\sqrt{N_m}$ , and extrapolated to x=0. Fit to  $\{1, x^{1/2}, x\}$ ,  $N_m^{\max}=15$ .

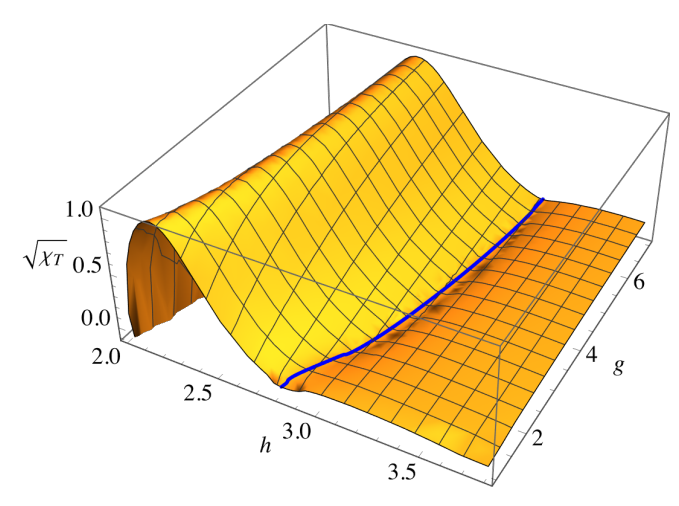


FIG. 9.  $\chi_T$  for  $N_m^{\rm max}=15$ ; in blue the critical line. We use the same approach as in Fig. 3 for  $\chi$ .

We now use  $\chi$ ,  $\chi_T$  and  $\chi_\sigma$  at  $N_m^{\rm max}=15$ , and repeat the analysis for the critical line and sweet spot. Fig. 12 shows this comparison, for a slightly coarser grid with  $\delta g=0.2$ ,  $\delta h=0.1$ . The resulting phase-transition lines lie close together, as do their sweet spots; deviations are well below the resolution of the computing grid. Our conclusion is that  $\chi$ ,  $\chi_T$  and  $\chi_\sigma$  give comparable results.

## G. Universality and $\mathcal{F}$ -function

The function  $\mathcal{F}$  in Eqs. (4) and (5) is universal, and recently values for it have been reported [31, 34]:

$$\mathcal{F}_{\rm free\ theory} = \frac{\ln(2)}{8} - \frac{3\zeta(3)}{16\pi^2} \simeq 0.0638071 \ [27]$$

$$\mathcal{F}_{\rm Ising}^{\rm fuzzy} = 0.0612(5) \ (\text{fuzzy sphere}) \ [31]$$

$$\mathcal{F}_{\rm Ising}^{4-\varepsilon} = 0.0610 \ (4-\varepsilon) \ [34] \ (17)$$

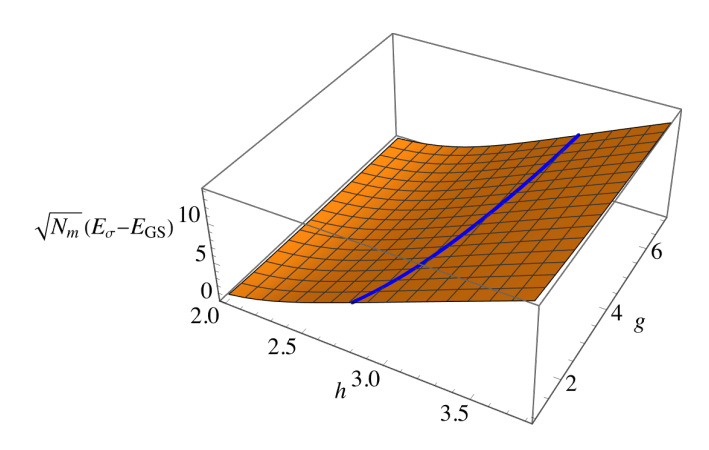


FIG. 10.  $\sqrt{N_m}(E_\sigma - E_{\rm GS})$  for  $N_m = 15$ . Note that the gap vanishes for small h: one is in the non-critical ferromagnetic phase.

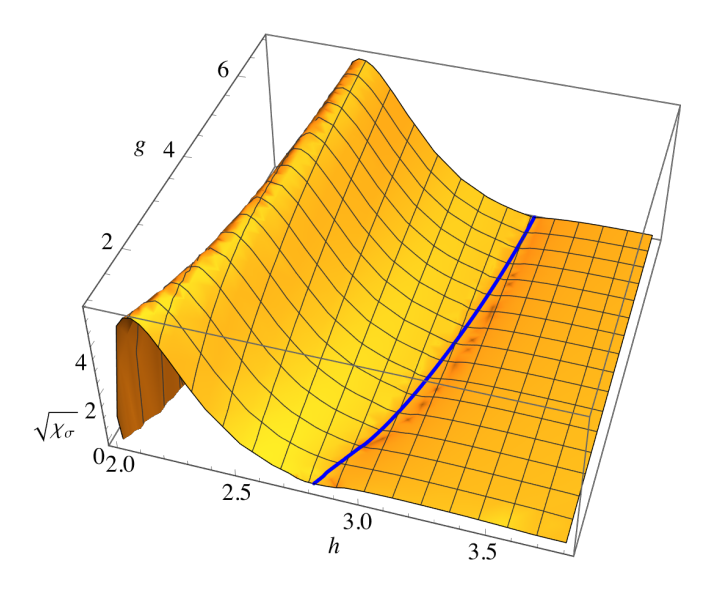


FIG. 11.  $\chi_{\sigma}$  for  $N_m^{\rm max}=15$ ; in blue the critical line. We use the same approach as in Fig. 3 for  $\chi$ , plotting the signed root  $\sqrt{\chi_{\sigma}}$ .

Can  $\mathcal{F}$  be accessed in our approach? An obvious guess is to take  $E_{3/2}$  in units of the stress-energy tensor<sup>3</sup>,

$$\mathcal{F} \stackrel{?}{=} 3\chi_T. \tag{18}$$

At size  $N_m = 15$ , we find for the sweet spot

$$3\chi_T \approx 0.00013$$
 at  $h = 3.16$ ,  $g = 4.51$ . (19)

This value is much smaller than  $\mathcal F$  reported in Eq. (17). It seems that in our approach  $\chi$  may even vanish, as we tested in Fig. 13: we evaluated  $\chi$  at the sweet spot of [1], using DMRG results for larger systems (the last point at  $N_m=23$  may not have converged.) By plotting both  $\chi$  and  $\chi\sqrt{N_m}$  we see

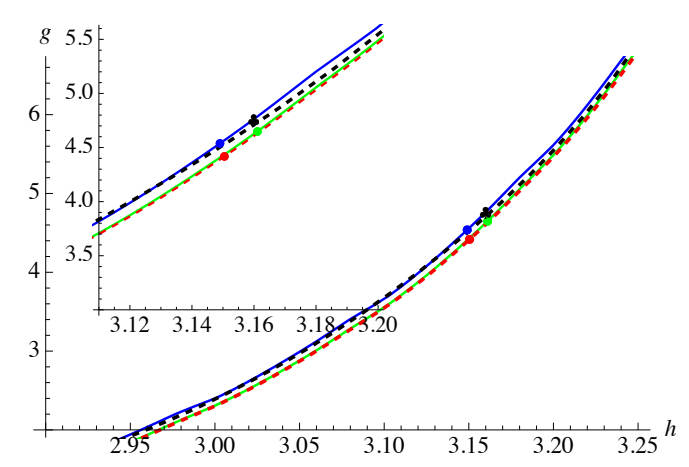


FIG. 12. As figure 6, with different denominators at size  $N_m^{\rm max} = 15$ :  $\chi$  (green),  $\chi_T$  (red dashed) and  $\chi_\sigma$  (blue). In black dashed the critical line of [1], a black trefel marking its sweet spot.

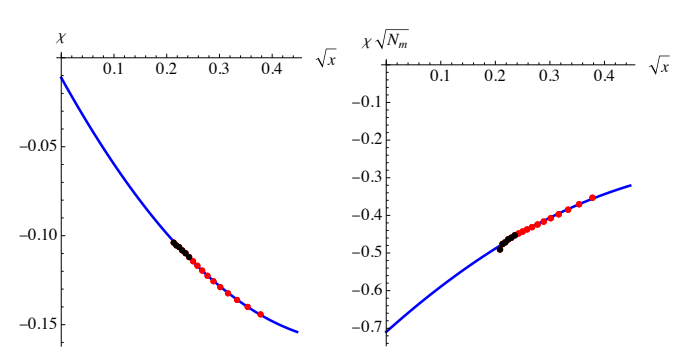


FIG. 13. Left:  $\chi$  as a function of  $\sqrt{x}$  for  $N_m$  ranging from  $N_m=6$  to  $N_m=23$ , at the sweet spot of [1], namely g=4.75, h=3.16. The black points are obtained via DMFT, and small numerical errors increase in the differences we take. (This is apparent in the last data point). To the right we show that the extrapolated value is so small, that it is consistent with a different scaling, namely that  $\chi\sqrt{N_m}$  converges for  $N_m\to\infty$ . All fits are quadratic polynomials in  $\sqrt{x}$ .

that this is consistent with  $\chi=0$  at the sweet spot. So either much larger system sizes are needed to extract  $\mathcal{F}$ , or  $\chi_T$  has no connection to  $\mathcal{F}$  and vanishes at the transition. This may not be too surprising, given that a quantum system on the fuzzy sphere is equivalent to  $S_2 \times \mathbb{R} = \mathbb{R}^3$ , and the latter should not have an anomaly.

## IV. CONCLUSION

We have shown how the phase-transition line on the fuzzy sphere, and the sweet spot of optimal conformality can be obtained from a finite-size analysis of the ground-state energy. This is achieved by analyzing the term of relative order  $N_m^{-3/2}$  in the ground-state energy, divided by the leading term, as a function of  $N_m$ . It yields the phase transition of [1] and their sweet spot with good precision. While small system sizes as  $N_m = 12$  already allow to locate the phase transition, the pre-

 $<sup>^3</sup>$  The number d=3 is the dimension of the stress-energy tensor.

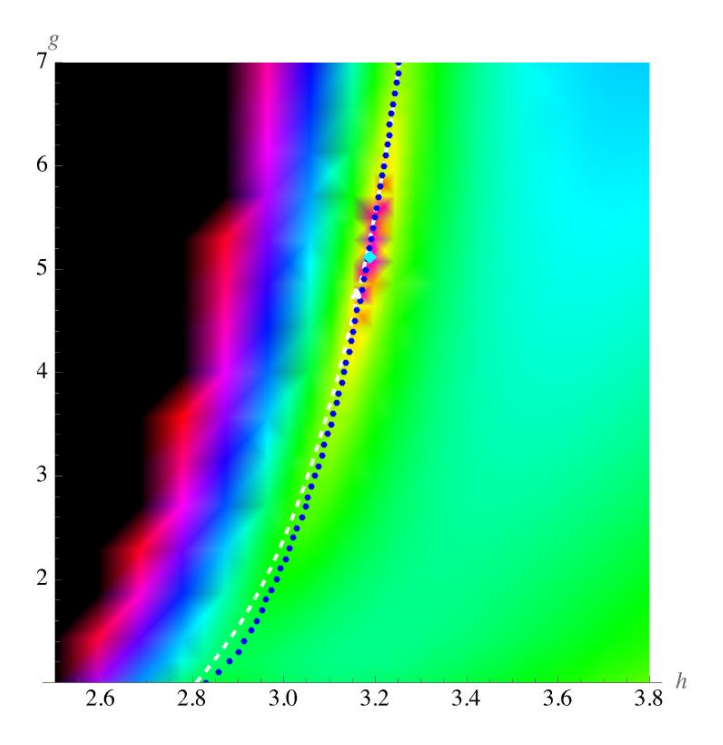


FIG. 14. The equivalent of Fig. 4, when using a polynomial in x of degree 4 for the fit, and analyzing  $-E_3/E_0$ .

cision increases for larger  $N_m$ . A non-negligible advantage of our approach is that it only requires to find the ground-state energy instead of the full spectrum, which is computationally fast: we need about 10 minutes for  $N_m=17$  on 8 cores.

To justify our procedure, one should compute the dependence of the ground-state energy around the sweet spot, i.e. CFT, following what has been done for dimension d=2 [35], and for the first excited states for the Ising CFT on the fuzzy sphere [33].

An alternative which does not normalize by the ground-state energy is to use either the stress-energy gap, or the gap of  $\sigma$ . Both procedures use a universal normalization, give comparable results, but are computationally slightly more costly.

We hope this procedure may prove useful for locating the critical point in models as the 3-state Potts model in dimension d=3, where the transition for real couplings is first-order [4–7]. Suppose we know an approximate location of the minimum in the real plane. We can then approximate  $\chi(h,g)$  by a polynomial around this point, and search for solutions of Eq. (14) in the complex plane, near the approximate mini-

mum.

## ACKNOWLEDGMENTS

The author thanks Slava Rychkov and Zheng Zhou for valuable discussions.

## Appendix A: Different extrapolation schemes

Since the term  $E_{3/2}$  seemingly vanishes at the transition, we can try to extract the phase-transition line from a fit to Eq. (9); reasonable agreement was achieved by considering the term of order 4, as is shown on Fig. 14. It finds the phase transition line, as well as the sweet spot, albeit with less precision. We do not know whether this somehow arbitrary procedure may have a use, but we wanted to point out that the proposed approach is rather robust.

A final mark of caution: when using Eq. (11) it is important to not terminate the expansion at  $E_{3/2}$ , but to keep the two following coefficients  $E_2$  and  $E_{5/2}$ . Dropping the latter still allows one to see the phase transition, albeit only at large  $N_m$ , and with less precision; the sweet spot moves to h=3.2, g=5.3. Dropping both terms gives a non-sensical result.

## **CONTENTS**

I.	Introduction	1
Π.	Size-dependence of the ground state energy	1
III.	Finite-size scaling analysis of the ground-state energy A. Model B. FuzzifiED C. Dependence of the ground-state energy on system	2 2 2
	<ul> <li>Dependence of the ground-state energy on system size</li> <li>D. Implementation</li> <li>E. Results for the location of the critical point</li> <li>F. Different normalizations</li> <li>G. Universality and F-function</li> </ul>	2 3 4 4 5
IV.	Conclusion	6
	Acknowledgments	7
A.	Different extrapolation schemes	7
	References	7

<sup>[1]</sup> W. Zhu, C. Han, E. Huffman, J.S. Hofmann and Y.-C. He, *Uncovering conformal symmetry in the 3d Ising transition: State-operator correspondence from a quantum fuzzy sphere regularization*, Phys. Rev. X **13** (2023) 021009.

<sup>[2]</sup> Z. Zhou and Y.-C. He, A new series of 3d CFTs with  $\mathrm{Sp}(n)$  global symmetry on fuzzy sphere, (2024), arXiv:2410.00087.

<sup>[3]</sup> Z. Zhou, C. Wang and Y.-C. He, Chern-Simons-matter

conformal field theory on fuzzy sphere: Confinement transition of Kalmeyer-Laughlin chiral spin liquid, (2025), arXiv:2507.19580.

<sup>[4]</sup> S. Yang, Y.-G. Yue, Y. Tang, C. Han, W. Zhu and Y. Chen, Microscopic study of 3d Potts phase transition via fuzzy sphere regularization, Phys. Rev. B 112 (2025) 024436, arXiv:2501.14320.

- [5] E.A. Cruz, I.R. Klebanov, G. Tarnopolsky and Y. Xin, Yang-Lee quantum criticality in various dimensions 2025, arXiv:2505.06369.
- [6] Y.-M. Sun, W.-J. Yu, X.-Y. Wang and L.-J. Zhai, Hybrid scaling mechanism of critical behavior in the overlapping critical regions of classical and quantum Yang-Lee edge singularities, (2025), arXiv:2506.00919.
- [7] J.E. Miro and O. Delouche, Flowing from the Ising model on the fuzzy sphere to the 3D Lee-Yang CFT, (2025), arXiv:2505.07655.
- [8] M. Reehorst, S. Rychkov, D. Simmons-Duffin, B. Sirois, N. Su and B. van Rees, *Navigator function for the conformal boot*strap, SciPost Phys. 11 (2021) 072.
- [9] D. Poland, S. Rychkov and A. Vichi, The conformal bootstrap: Theory, numerical techniques, and applications, Rev. Mod. Phys. 91 (2019) 015002.
- [10] S. El-Showk, M. F. Paulos, D. Poland, S. Rychkov, D. Simmons-Duffin and A. Vichi, Solving the 3d Ising model with the conformal bootstrap ii. c-minimization and precise critical exponents, J. Stat. Phys. 157 (2014) 869–914, arXiv:1403.4545.
- [11] S. El-Showk, M.F. Paulos, D. Poland, S. Rychkov, D. Simmons-Duffin and A. Vichi, Solving the 3D Ising model with the conformal bootstrap, Phys. Rev. D 86 (2012) 025022.
- [12] S.M. Chester, W. Landry, J. Liu, D. Poland, D. Simmons-Duffin and A. Vichi N. Su, Carving out ope space and precise O(2) model critical exponents, (2019), arXiv:1912.03324.
- [13] G. Fardelli, A.L. Fitzpatrick and E. Katz, Constructing the infrared conformal generators on the fuzzy sphere, (2024), arXiv:2409.02998.
- [14] R. Fan, Note on explicit construction of conformal generators on the fuzzy sphere, (2024), arXiv:2409.08257.
- [15] H.W.J. Blöte, J.L. Cardy and M.P. Nightingale, Conformal invariance, the central charge, and universal finite size amplitudes at criticality, Phys. Rev. Lett. 56 (1986) 742–745.
- [16] J. Cardy, Conformal invariance and statistical mechanics, in E. Brézin and J. Zinn-Justin, editors, Fields, strings and critical phenomena, Volume XLIX of Les Houches, école d'été de physique théorique 1988, North Holland, Amsterdam, 1988.
- [17] J.L. Jacobsen and K.J. Wiese, Lattice realization of complex CFTs: Two-dimensional Potts model with Q > 4 states, Phys. Rev. Lett. 133 (2024) 077101, arXiv:2402.10732.
- [18] A.B. Zamolodchikov, "Irreversibility" of the flux of the renormalization group in a 2D field theory, Pis'ma Zh. Eksp. Theor.

- Fiz. 43 (1986) 565-567, JETP Lett. 43 (1986) 730.
- [19] S. Deser and A. Schwimmer, Geometric classification of conformal anomalies in arbitrary dimensions, Phys. Lett. B 309 (1993) 279–284.
- [20] M.J. Duff, Twenty years of the Weyl anomaly, Classical and Quantum Gravity 11 (1994) 1387.
- [21] Z. Komargodski and A. Schwimmer, On renormalization group flows in four dimensions, JHEP 2011 (2011) 99.
- [22] J.L. Cardy, *Is there a c-theorem in four dimensions?*, Phys. Lett. B **215** (1988) 749–752.
- [23] H Casini and M Huerta, Entanglement entropy in free quantum field theory, J. Phys. A 42 (2009) 504007.
- [24] D.L. Jafferis, I.R. Klebanov, S.S. Pufu and B.R. Safdi, *Towards the F-theorem:*  $\mathcal{N}=2$  *field theories on the three-sphere*, JHEP **2011** (2011) 102.
- [25] R.C. Myers and A. Sinha, Holographic c-theorems in arbitrary dimensions, JHEP 2011 (2011) 125, arXiv:1011.5819.
- [26] D.L. Jafferis, The exact superconformal R-symmetry extremizes Z, JHEP 2012 (2012) 159, arXiv:1012.3210.
- [27] I.R. Klebanov, S.S. Pufu and B.R. Safdi, F-theorem without supersymmetry, JHEP 2011 (2011) 38, arXiv:1105.4598.
- [28] M.P. Hertzberg and F. Wilczek, Some calculable contributions to entanglement entropy, Phys. Rev. Lett. 106 (2011) 050404.
- [29] H. Liu and M. Mezei, A refinement of entanglement entropy and the number of degrees of freedom, JHEP 2013 (2013) 162, arXiv:1202.2070.
- [30] H. Casini and M. Huerta, Renormalization group running of the entanglement entropy of a circle, Phys. Rev. D 85 (2012) 125016
- [31] L. Hu, W. Zhu and Y.-C. He, Entropic F-function of 3D Ising conformal field theory via the fuzzy sphere regularization, (2024), arXiv:2401.17362.
- [32] Z. Zhou, Fuzzified: Julia package for numerics on the fuzzy sphere, (2025), arXiv:2503.00100.
- [33] A.M. Läuchli, L. Herviou, P.H. Wilhelm and S. Rychkov, Exact diagonalization, matrix product states and conformal perturbation theory study of a 3d Ising fuzzy sphere model, (2025), arXiv:2504.00842.
- [34] S. Giombi and I.R. Klebanov, *Interpolating between a and F*, JHEP 2015 (2015) 117.
- [35] A.W.W. Ludwig and J.L. Cardy, Perturbative evaluation of the conformal anomaly at new critical points with applications to random systems, Nucl. Phys. B 285 (1987) 687–718.